Operational Implementation of the ATOVS Processing Procedure in KMA and Its Validation P4 A

Myoung-Hwan AHN*, Mee-Ja KIM, Chu-Yong CHUNG, and Ae-Sook SUH

Remote Sensing Research Laboratory/Meteorological Research Institute, Seoul 156-720, *Korea*

(Received June 8, 2002; revised January 21, 2003)

ABSTRACT

The Korea Meteorological Administration (KMA) has processed the data from the advanced TOVS (ATOVS) onboard NOAA-16 satellite since May 2001. The operational production utilizes the AAPP (ATOVS and AVHRR Processing Package) of EUMETSAT and IAPP (International ATOVS Processing Package) of the University of Wisconsin. For the initial guess profiles, the predicted fields (usually 6 to 12 hour forecasted fields) from the global aviation model of NOAA/NCEP are used. The average number of profiles retrieved from the ATOVS data is about 1,300 for each morning and afternoon orbit at about 18 and 06 UTC, respectively. The retrieved temperature and dew point temperatures are provided to forecasters in real time and used for initialization of prediction models. With the advanced microwave sensor (AMSU; Advanced Microwave Sounding Unit), accuracy of the ATOVS products is expected to be better than that of the TOVS products, especially in cloudy conditions. Indeed, the preliminary results from a validation study with the collocated radiosonde data during a 8-month period, from May to December 2001, for the East Asia region show an improved accuracy of the ATOVS products for cloudy skies versus the TOVS, especially for higher altitudes. The RMS (Root Mean Square) difference between the ATOVS products and radiosonde data is about 1.3°C for both clear and cloudy conditions, except for near the ground and at higher altitudes, at around 200 hPa. There is no significant temporal variation of the error statistics at all pressure levels. In case of the water vapor mixing ratio, the largest difference is shown at lower altitudes, while the accuracy is much better for the clear sky cases than the cloudy sky cases. The bias and RMSE at lower altitudes is about 0.557 g kg^{-1} and 2.5 g kg^{-1} and decrease significantly with increasing altitude.

Key words: ATOVS Processing and validation, temperature and humidity profiles

1. Introduction

The vertical profiles of temperature and humidity retrieved from satellite observations have played important roles both in the analysis of current weather conditions and in the prediction of the future status of the atmosphere (Smith et al., 1985; Menzel and Chedin, 1990). The importance of satellite derived soundings for improving accuracy of the numerical weather prediction models is especially exemplified through the providing of information for data-sparse regions, such as over the ocean (Le Marshall et al., 1989, 1995). The actual retrieval of soundings from satellite observed thermal emission requires the inverse solution of the atmospheric radiative transfer equation (RTE). Due to several reasons, such as the overlapping of a broad weighting function and instrument noise, a unique solution for the sounding is not available (Fleming and Smith, 1971; Rodgers, 1976). As a consequence, there are many indirect approaches to solve the inverse problem, which include the relaxation method (Chahine, 1968, 1970; Barcilon, 1975), iterative method (Smith, 1970), inverse matrix method (Smith and Woolf, 1976), and physical iteration method (Smith et al., 1993; Li et al., 2000).

In 2000, the second satellite of the advanced NOAA (National Oceanic and Atmospheric Agency) polar orbiting satellites, NOAA-16, was launched successfully, and the operational distribution of data started in April 2001. The second generation of the NOAA polar orbiting weather satellites, beginning with the NOAA-15 launched in May 1998, is meant to replace the first generation NOAA/TIROS-N polar orbiting weather satellite system. The new system is composed of two sun-synchronous polar orbiting spacecraft, one of which is in a morning orbit (AM), the second is in

*E-mail: mhahn@kma.go.kr

an afternoon (PM) orbit. NOAA-15 is for the morning orbit, while the NOAA-16 flies the afternoon orbit. Recently, NOAA-17 was launched to replace the NOAA-15, which suffered from several instrumentation and communication problems.

One of the important changes in the instrumentation of the new satellite series is the improved sounding capability. The replacement of the Stratospheric Sounding Unit (SSU) and the Microwave Sounding Unit (MSU) of the first generation by the Advanced Microwave Sounding Units (AMSU-A with 15 channels and AMSU-B with 5 channels) is the most notable improvement. The AMSU instruments represent a nearly all-weather capability to compute soundings of atmospheric and surface conditions on a global basis. Inclusion of the AMSU instrument is expected to improve retrievals in cloudy and partly cloudy regions. In addition, the capability to detect precipitation, ice and snow on the surface is also expected to show a significant improvement (Weng and Grody, 2000).

The main instrument for sounding in the infrared (IR) radiation region is almost the same for the two generations. The High Resolution Infrared Radiation Sounder (HIRS/2) onboard the first generation remains nearly unchanged in the HIRS/3 on the second generation NOAA series. The instrument package is complemented by the Advanced Very High Resolution Radiometer (AVHRR/3) which replaces AVHRR/2 of the TIROS-N satellites which provide image data in the visible and infrared spectral regions. The higher resolution AVHRR image data can provide improved accuracy in cloud detection within the HIRS field of view.

The data processing procedure, from calibration to the actual retrieval, for vertical temperature and humidity retrieval consists of two freely available software packages. The AAPP (AVHRR and ATOVS Processing Package) of EUMETSAT and International ATOVS (Advanced TIROS Operation Vertical Sounder) Processing Package (IAPP) of the University of Wisconsin are the de facto standard packages to process the real-time direct broadcast HRPT (High Resolution Picture Transmission) data from the new generation NOAA polar orbiting satellites (Li et al., 2000). AAPP is used for the initial processing of the HRPT such as navigation, calibration, decommutation, and preliminary cloud screening, while the IAPP is for the actual retrieval of profiles. IAPP uses either a statistical regression method (Smith et al., 1970) or a model predicted field to provide the first-guess profile. With the first guess and other auxiliary data, IAPP adopts a physical iterative algorithm for the actual retrieval. The statistical first guess is derived from a climatological dataset archived by the LMD (Laboratoire de Meteorologie Dynamique) and is called "TIGR (Thermodynamic Initial Guess Retrieval)" statistical data.

The basic products from the IAPP are vertical profiles of temperature, water vapor mixing ratios at 42 standard pressure levels from the ground to 0.1 hPa, and the total column ozone. Currently, the spatial resolution is about 90× 90 km which corresponds to the 3×3 instantaneous field of view (IFOV). The derived products from the basic products are geopotential height, stability index, gradient, and geostrophic winds (Li et al., 2000). After installation of AAPP and IAPP, the Korea Meteorological Administration (KMA) has had ATOVS products in operation since May 2001. The final products from the current system can be produced within 1 hour of the reception of the raw HRPT data.

The current study introduces the operational ATOVS processing system in KMA and shows the validation results of temperature and relative humidity for a rather short time period, about 8 months, for the limited area over the East Asia region. The preliminary validation results encourage the use of ATOVS products in real-time weather analysis and numerical prediction models. A brief introduction of the basic principles of the retrieval is given in section 2, followed by an explanation of the operational routines for data processing and actual retrieval of the new packages in section 3. Section 4 gives the validation results with a brief explanation of the raw satellite data and radiosonde observation. This paper is concluded in section 5.

2. Retrieval of vertical temperature and moisture

The infrared monochromatic radiance measured at the top of the atmosphere as a function of the pressure coordinate can be denoted (neglecting the scattering by large particles and contribution by the IR portion of solar radiation) as

$$I_v(p=0) = \varepsilon I_v(p_s)K(p_s) + \int_{p_s}^{0} B_v[T(p)]\frac{\partial K_v(p)}{\partial p}dp - (1-\varepsilon)\int_{p_s}^{0} B_v[T(p)]\frac{\partial K_v^*(p)}{\partial p}dp, \quad (1)$$

where $I_v(p=0)$ is the radiance reaching the top of the atmosphere, $I_v(p_s)$ is the radiance emitted from the surface (pressure is p_s) by assuming a blackbody surface, $K_v(p)$ is the monochromatic transmittance from a pressure level p to the top of the atmosphere, and $B_v[T(p)]$ is the Planck function representing the radiance emitted by the air with temperature (T) at pres-

sure p. Terms ε and $K_v^*(p)$ are the surface emissivity and transmittance in between pressure level p and the surface multiplied by the transmittance between the surface and the top of the atmosphere.

The physical meaning of the first term on the right hand side of Equation (1) is the radiance portion that comes from the surface emission attenuated by the atmosphere between the surface and the top of the atmosphere. The second term is the contribution from the emission of the atmospheric layer below the satellite altitude. Finally, the third term is the downward atmospheric radiation reflected by the surface. The gradient of transmittance from a given pressure p to the top of the atmosphere in the second term is called the weighting function because it weights the atmospheric emission $B_v[T(p)]$ term. It is well known that the weighting function is closely related with the maximum information contents (Mateer, 1965; Rodgers, 1976).

The transmittance function is dependent on temperature and the mixing ratio of the absorbing gases, and can be defined as

$$K_v(p) = e^{-\tau} = \exp\left[-\frac{1}{g}\int_0^p k_v(p')q(p')dp'\right], \quad (2)$$

where τ is the optical depth, g is the gravitational constant, k_v is the absorption coefficient, and q is the mixing ratio of the absorbing gas. Thus, for the retrieval of the temperature sounding, it is convenient to use the wavelength bands in which the measured radiance at the top of the atmosphere are sensitive to the relatively homogeneous and uniformly distributed gases, such as carbon dioxide and oxygen. The carbon dioxide absorption bands at 4.3 μm and 15 μm are extensively used for the IR temperature sounding while the 150 GHz oxygen absorption bands are used for the microwave temperature soundings. On the other hand, the concentration of trace gases, such as water vapor and ozone, is retrieved from the radiance measured at the wavelengths which are sensitive to the gas absorption, provided the temperature profile is already prepared. For example, the humidity is derived from the water vapor absorption band, near 6.3 μm and 183 GHz for the infrared and microwave regions, respectively.

For the actual satellite observation, the band-averaged radiances instead of the monochromatic radiances are measured and Equation (1) should be integrated over the wavelength using the spectral response function for each channel. The mathematical expression for the band-averaged radiance is identical with that of the monochromatic, in so far as the physical parameters are band-averaged quantities:

$$\overline{K}_v(p) = \frac{\int_{v_1}^{v_2}\phi(v)\,K_v(p)\,dv}{\int_{v_1}^{v_2}\phi(v)\,dv}, \quad (3)$$

$$\frac{\partial\overline{K}_v(p)}{\partial p} = \frac{\int_{v_1}^{v_2}\phi(v)\,\dfrac{\partial K_v(p)}{\partial p}\,dv}{\int_{v_1}^{v_2}\phi(v)\,dv}. \quad (4)$$

The essence of the retrieval of the temperature profile from a set of observed radiances is obtaining the inverse solution of Equation (1), which is well-known as the first kind of Fredholm equation. The solution is naturally unstable because $I_v(p{=}0)$ is the measured values with observation errors, and the weighting function is not an ideal Dirac-delta function (Fleming, 1977; Strand and Westwater, 1968). Thus, to get a stable solution, we need to measure the radiance as accurately as possible, select bandwidth as sharply as possible, and find the most stable methods to solve the inverse problem. With certain limitations in the engineering part of the retrieval problems, many different mathematical approaches have been developed (Rodgers, 1976; Deepak et al., 1985; Twomey, 1963). Rodgers (1976) gives a nice summary of several statistical and physical retrieval methods developed for the actual application of Equation (1).

The IAPP developed for the ATOVS products adopts the non-linear physical iteration method (Smith et al., 1993; Li et al., 2000), which linearizes the radiative transfer equation using the perturbation theorem. The minimum variance solution is obtained by minimizing the penalty function (Rodgers, 1976). A detailed explanation of the retrieval algorithm can be found elsewhere (Li et al., 2000; Li and Huang, 1999). Here we briefly introduce the necessary equations pertinent for a later explanation of the algorithm. Following Li et al. (2000), Equation (1) can be linearized using the perturbation theorem to

$$\delta T_{\rm B} = W_{\rm Ts}\delta T_{\rm s} + \int_{p_{\rm s}}^{0} W_{\rm T}\delta T dp + \int_{p_{\rm s}}^{0} W_q\delta\ln q dp + W_\varepsilon\delta\varepsilon, \quad (5)$$

where $T_{\rm B}$ is the brightness temperature, and $W_{\rm Ts}$, $W_{\rm T}$, W_q, and W_ε are the weighting functions of surface temperature, atmospheric temperature, water vapor, and surface emissivity, respectively. In practice, the emissivity term is only important for the microwave channel data, and Equation (5) holds for all ATOVS

observation channels and can be rewritten in a vector form as

$$\delta \boldsymbol{y} = F' \boldsymbol{x}, \tag{6}$$

where $\boldsymbol{y}$ denotes the vector of the observed brightness temperature at N channels, and $\boldsymbol{x}$ denotes the vector for the unknown parameters such as the temperature and water vapor profiles. The regularization solution of Equation (6) can be obtained as follows when the background error covariance is not known or is a non-Gaussian distribution, by minimizing the penalty function (Rodgers, 1976):

$$J(\boldsymbol{x}) = [\boldsymbol{y}_o - \boldsymbol{y}(\boldsymbol{x})]^{\mathrm{T}} \boldsymbol{E}^{-1} [\boldsymbol{y}_o - \boldsymbol{y}(\boldsymbol{x})] + [\boldsymbol{x} - \boldsymbol{x}_0]^{\mathrm{T}} \boldsymbol{H} [\boldsymbol{x} - \boldsymbol{x}_0], \tag{7}$$

where $\boldsymbol{y}_o$ and $\boldsymbol{y}(\boldsymbol{x})$ are the observed and estimated brightness temperatures, respectively, while $\boldsymbol{x}_0$ is the initial guess value. $\boldsymbol{E}$ is the observation error covariance matrix including both the instrument noise and forward model error, while $\boldsymbol{H}$ is for the expected background error covariance matrix. The superscript T represents the transpose of the vector. The maximum likelihood solution of Equation (7) can be obtained if the observation and first guess profile error covariance follow the Gaussian distribution:

$$\delta \boldsymbol{x} = \left(F_n'^t \boldsymbol{E}^{-1} F_n' + \gamma i \right) F_n'^t \boldsymbol{E}^{-1} \times \left(\delta \boldsymbol{y}_n + F_n' \delta \boldsymbol{x}_n \right). \tag{8}$$

Li et al. (2000) adopted a dynamic approach to determine the smoothing factor γ which varies at each iteration for IAPP.

3. Operational procedure

The overall ATOVS processing procedures implemented in KMA are summarized in Fig. 1, which runs from the extraction of the raw data to the quality control of the derived products. The package consists of three major modules: pre-processing, retrieval procedure, and post-processing. The pre-processing includes the processes of ingestion, navigation, calibration, mapping, and cloud mask. These processes are conducted by the AAPP package, which has been developed by EUMETSAT with participation from several European space agencies. The data from a successful application of AAPP is called level 1d, which contains the AMSU brightness temperature interpolated into each HIRS/3 FOV along with the HIRS/3 brightness temperature, a preliminary cloud screening result. The actual simultaneous retrieval of temperature and humidity profiles is made by IAPP which uses the level 1d data and other auxiliary data such as the model first guess field, surface observation data, and upper air observation. Finally, the output file written in NetCDF format (http://www.unidata.ucar.edu/packages/netcdf/) contains the derived vertical profiles of temperature, humidity, first guess temperature, total column ozone, and total precipitable water.

3.1 *AAPP*

The AAPP procedure starts with the update of the orbital information of the satellite from the TBUS message, which is available on the GTS (Global Telecommunication System) circuit. Within the TBUS message, the predicted orbital parameters for the specific location, time, and satellite are used to determine the real-time satellite position when the data is received. Once the position is determined, the extraction of level 0 data at a given geographical position for each instrument is performed by decommutation of raw HRPT data. Current ATOVS/HRPT contains the AVHRR data, the TIP (TIROS Information Processor) and/or the AIP (ATOVS Information Processor) data, which include HIRS/3, and AMSU

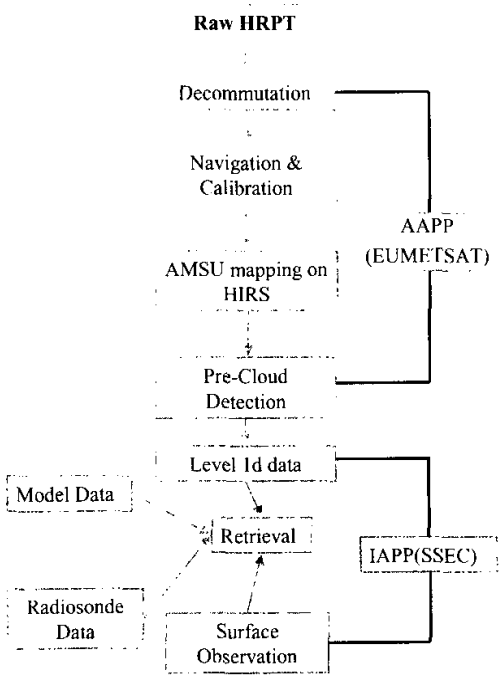

Fig. 1. The overall flow chart for the KMA ATOVS processing procedure. Pre-processing is done by using the AAPP package and the retrieval is performed using the IAPP package with the initial guess fields from the NOAA/NCEP Aviation model.

data with other instrument data such as SBUV. For the ATOVS process, both the AVHRR and AIP data are decommutated and stored in a separate file for each instrument as level 1b files.

With the instrument information such as the scan rate, the number of fields of view within a scan and the correct position of an instrument scan pixel for each instrument on the Earth's surface is estimated. For each instrument, radiance values are further processed for navigation and earth location, and calibration. The calibration procedure extracts the onboard calibration parameters (e.g., blackbody count, space counts, etc.) from the data stream, estimates the calibration coefficients using these counts (NOAA, 1988), and finally applies these calibration coefficients to the actual observation data, to transform them from binary units (counts) into physical parameters (brightness temperatures or radiances). Navigation and earth location procedures map all instrument data to a common position to be used in the actual retrieval using the information provided by the TBUS. The calibrated and navigated data are stored as the level 1c data files.

Finally, for simultaneous use of the three sounding instruments, both AMSU-A and AMSU-B radiance data are mapped into the HIRS/3 field of view. First, the AMSU-B data is mapped to AMSU-A FOV and then both AMSU-A and AMSU-B data are mapped to the HIRS FOV. After the re-mapping, sets of pre-procedures such as determination of precipitation and/or cloudy areas and limb corrections could be performed. Currently, as these processes are extensively performed in IAPP, we do not perform these tests. The final product from the AAPP procedure is the calibrated, mapped, and geo-located data in a single level 1d file, which can be used for input in the actual retrieval procedure or for direct assimilation into a numerical model.

3.2 *IAPP*

Actual temperature and moisture soundings are derived from the second package, IAPP developed by the SSEC/University of Wisconsin (Li et al., 2000). The IAPP and its predecessor, the International TOVS Processing Package (ITPP), have been developed to retrieve atmospheric temperature and moisture profiles, total ozone, and other parameters in both clear and cloudy atmospheres from ATOVS/TOVS radiance measurements. The IAPP currently uses radiances from HIRS/3, AMSU-A, and AMSU-B preprocessed by AAPP into the level 1d data format for retrieval. Ancillary data inputs for retrieval include medium-resolution topography (0.167° latitude× 0.167° longitude) data supplied in the package, upper air observations, surface observations, and/or numerical model data. If surface observations are not available, numerical model data is used to define surface conditions; or, when neither is available, window channel radiances are used to best approximate surface conditions. The current study uses the outputs from the numerical model, NCEP/Aviation model, which also provides the first guess fields of temperature and moisture profiles. After reading the necessary input files, the retrieval is made through four steps: (1) cloud detection and estimation of clear sky radiance; (2) bias adjustment; (3) regression retrieval; and (4) nonlinear iterative physical retrieval (Li et al., 2000). Depending on the presence of clouds, a HIRS+AMSU-A+AMSU-B retrieval, AMSU-A+AMSU-B only retrieval, or no retrieval is made for each 3 × 3 HIRS FOV matrix. The cloud detection and retrievals are made on a 9-pixel box to enhance the data quality through a better determination of the cloud contamination and estimation of the clear sky radiance, and by reduction of the instrument noise. At present, the bias correction is not applied because the correction parameter is not temporally and spatially adjusted (Li, 2002, private communication).

For the cloud detection, two kinds of different tests, a series of the threshold tests and inter-comparison between HIRS and AMSU window channels, are applied. For the threshold test, if the root mean square (RMS) difference of HIRS and AMSU brightness temperature within the 3×3 FOVs is less than the pre-determined threshold value, it is then assumed that some of the FOVs are cloud free. The pre-determined threshold value is 3 times the instrument noise shown in Table 1. Otherwise, the RMS difference is recalculated after removing one FOV, which has the largest negative deviation from the averaged brightness temperature. If the re-calculated RMS difference satisfies the criteria, the clear sky radiances are assumed to be the re-calculated radiances. The procedure is repeated if it does not satisfy the criteria until only two FOVs remain. If the RMS difference does not satisfy the criteria with the remaining two FOVs, profiles are not obtained. The next step is the comparison between the estimated HIRS channel-8 (11 μm window channel) brightness temperature, which is obtained from the regression of AMSU window channel brightness temperature, and the measured HIRS channel-8 brightness temperature. If the difference between the estimated and measured brightness temperature is more than 3 degrees, the FOV is assumed to be contaminated by clouds. The radiances used for the retrieval are the averaged radiances for all of the clear sky FOVs within the 9 pixels.

Table 1. The center wavelength of NOAA-16/HIRS channels and frequencies for AMSU channels and the noise values in units of K (NOAA, 1998)

Channel	HIRS/3		AMSU	
	Center Wavelength (μm)	Noise (K)	Center Frequency (GHz)	Noise (K)
1	14.95	1.20	23.8	1.14
2	14.71	0.33	31.4	1.05
3	14.49	0.33	50.3	1.50
4	14.22	0.33	52.8	0.30
5	13.97	0.39	53.6	0.30
6	13.64	0.42	54.4	0.30
7	13.35	0.54	54.9	0.24
8	11.11	0.54	55.5	0.24
9	9.71	0.63	57.29	0.24
10	12.47	0.54	57.29±0.217	0.24
11	7.33	0.54	57.29±0.322±0.048	0.24
12	6.52	1.47	57.29±0.322±0.022	0.33
13	4.57	0.54	57.29±0.322±0.010	0.48
14	4.52	0.60	57.29±0.322±0.045	0.51
15	4.47	0.60	89.0	0.54
16	4.45	0.71	89.0	0.96
17	4.13	0.33	150.0	1.20
18	4.00	0.33	183.3±1.00	0.69
19	3.76	0.33	183.3±3.00	1.56
20	0.690		183.3±7.00	0.93

For the first guess profile, we use the model-predicted parameters from the NCEP Aviation model. Although the physical iterative retrieval is less dependent on the first guess profile compared to the regression methods, an accurate first guess is always better for improved accuracy in the retrieved profiles. The NCEP Aviation model is usually available at 0340 UTC and 1532 UTC for a 6-hour forecasting field. Currently the top atmosphere used in the IAPP is 20 hPa and the total number of levels is 26.

Physical iterative retrieval uses the measured and estimated brightness temperature for the determination of convergence. To estimate the brightness temperature, IAPP uses the surface emissivity, temperature profiles, and water vapor and ozone concentration together with a simplified radiative transfer model. The choice of the number of channels used for the retrieval varies with the instrument noise values monitored in real-time at NOAA/NESDIS. For the current study, we use the HIRS/3 channels from 1 to 17, AMSU-A channels from 3 to 14, and AMSU-B channels from 17 to 20. The iteration stops when the RMS values of the brightness temperature difference between the measured and estimated value are smaller than those of previous calculations and when the number of iterations is more than 5. On the other hand, if the RMS value increases more than 3 times during the iteration or the number of iterations is more than 5 and there is still no convergence, then the final values are assumed to be the same as the first guess.

4. Validation

4.1 *Data*

After the launch of the first polar orbiting meteorological satellite on 1 April 1960, the first operational polar orbiter was launched on 15 October 1972 and soon after was named NOAA-2. The NOAA series has been successfully operated since then and a summary of the series is shown in Table 2. Since NOAA-6, the vertical profile of temperature and humidity is obtained by using the TOVS, consisting of HIRS, MSU, and SSU which have 20, 4, and 3 channels, respectively

(Smith et al., 1979). As mentioned earlier, the second generation of NOAA polar orbiting satellites began with the NOAA-15 satellite launched on 13 May 1998. The major improvement of the second generation is the use of the advanced microwave sensor, AMSU, which consists of two different instruments, AMSU-A and AMSU-B. AMSU-A measures microwave radiances at 15 channels, frequencies between 22 and 89 GHz, to mainly derive vertical profiles of temperature using the oxygen absorption bands, around 54 GHz. AMSU-B measures radiances at 5 channels, from 89 GHz to 183 GHz, for the retrieval of the water vapor profile using the 183 GHz water vapor absorption frequencies. The AMSU scans cross track with an angle of ±48.95° (NOAA, 1998). The spatial resolutions of AMSU-A and AMSU-B are about 50 km and 15 km at nadir. On the other hand, the infrared sounding instrument has not changed significantly from the first generation to the second generation. HIRS/3 onboard the second-generation satellite also scans cross track with a scan angle of ±49.5° covering about ±1125 km at the ground. The spatial resolution at nadir is about 17.4 km and increases toward the far scan position, 58.5 km at farthest position (NOAA, 1998). HISR/3 covers the whole Earth twice a day.

Table 2. A series of NOAA polar orbiting satellites and their launch dates, operation periods, and orbit types. NOAA-M was launched on 24 June 2002

Series	Launch Date	Mission End Date	Orbit	Remarks
NOAA-1	Dec. 11, 1970	Aug. 19, 1971	Sun-Sync	VHRR
NOAA-2	Oct. 15, 1972	Jan. 30, 1975	Sun-Sync	VHRR
NOAA-3	Nov. 6, 1973	Aug. 31, 1976	Sun-Sync	VHRR
NOAA-4	Nov. 15, 1974	Nov. 18, 1978	Sun-Sync	VHRR
NOAA-5	July. 29, 1976	Jul 16, 1979	Sun-Sync	VHRR
TIROS-N	Oct. 13, 1978		Sun-Sync	AVHRR, HIRS, MSU, SSU
NOAA-A(6)	Jun 27, 1979	Mar. 31, 1987	Sun-Sync	TOVS
NOAA-B	May 29, 1980	Failed		
NOAA-C(7)	Jun 23, 1981	Jun 1986	Near-Polar	
NOAA-E(8)	Mar. 28, 1983	Dec. 29, 1985		
NOAA-F(9)	Dec. 12, 1984	Feb. 13, 1988	Near-Polar	TOVS failed Mar. 1987
NOAA-G(10)	Sep. 17, 1986		Near-Polar	
NOAA-H(11)	Sep. 24, 1988		Near-Polar	
NOAA-D(12)	May 14, 1991	Present	Near-Polar	
NOAA-I(13)	Aug. 9, 1993	Aug. 21, 1993	Near-Polar	Power failure
NOAA-J(14)	Dec. 20, 1994	Present	Near-Polar	
NOAA-K(15)	May 13, 1998	Present	Near-Polar	ATOVS
NOAA-L(16)	Sep. 21, 2000	Present	Near-Polar	ATOVS
NOAA-M(17)	Jun 24, 2002	Present	Near-Polar	ATOVS
NOAA-N`			Near-Polar	

VHRR: Very High Resolution Radiometer, AVHRR: Advanced Very High Resolution Radiometer
HIRS: High resolution Infrared Sounder
MSU: Microwave Sounding Unit
SSU: Stratospheric Sounding Unit
AMSU: Advanced Microwave Sounding Unit
TOVS: TIROS (Television and Infrared Observational Satellite) Operational Vertical Sounder
ATOVS: Advanced TOVS

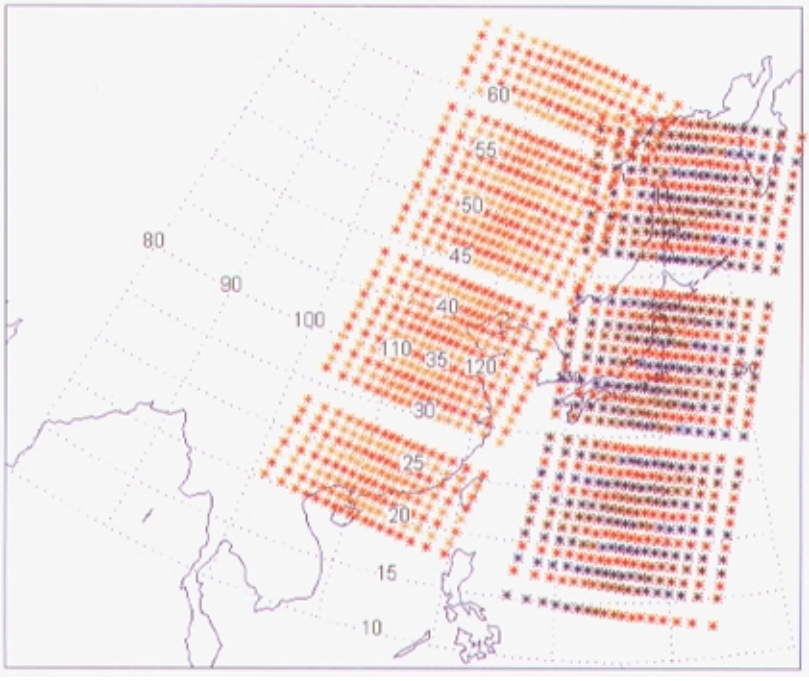

Fig. 2. The distribution of the retrieval points on 15 May 2001. The missing lines between the retrieved data are due to the calibration process. Across the scan, a total of 18 points are retrieved.

The data used for the current study is from the direct broadcast data of NOAA-16 received at the headquarters of KMA. Due to a frequent malfunctioning of instruments and the high noise signal of NOAA-15/AMSU data, we mainly use the NOAA-16 data for the current study. Since the installation of the new receiving/analysis system, MESDAS-2, in KMA the stability of data reception and speed of data analysis have dramatically improved. With the new system, all the pass data since the end of 1998 have been archived at the Satellite Meteorology Division of KMA. The typical coverage of NOAA-16 and the available retrieval information is shown in Fig. 2. The missing lines between the retrieved points are due to the calibration procedure for which the instrument measures the space and blackbody radiances (NOAA, 1998).

An example of the retrieved temperature and dew point distribution at 850 and 700 hPa is shown in Fig. 3 for 1800 UTC 14 July 2001, when a heavy rainfall occurred over the central Korean Peninsula. Here, the missing data points for the calibration are filled in through an optimal interpolation. The 850 and 700 hPa temperature fields show a well-developed temperature trough and baroclinicity located northwest of the central Korea Peninsula. At 850 hPa, a strong cold trough resides over the central peninsula, while the 700 hPa cold trough is located further northwest. Along with the temperature distribution, the dew point temperature shows a band of high moisture area over central Korea both at 850 and 700 hPa. The dew point gradient is also very strong along the central part of the Peninsula. With the strong southwestly flow of moist air into the Peninsula, heavy rainfall caused a severe flash flood over the central peninsula. As the upper air observation data at the 1800 UTC time slot is not readily available, profiles derived from NOAA-16 play an important role in short-range forecasting.

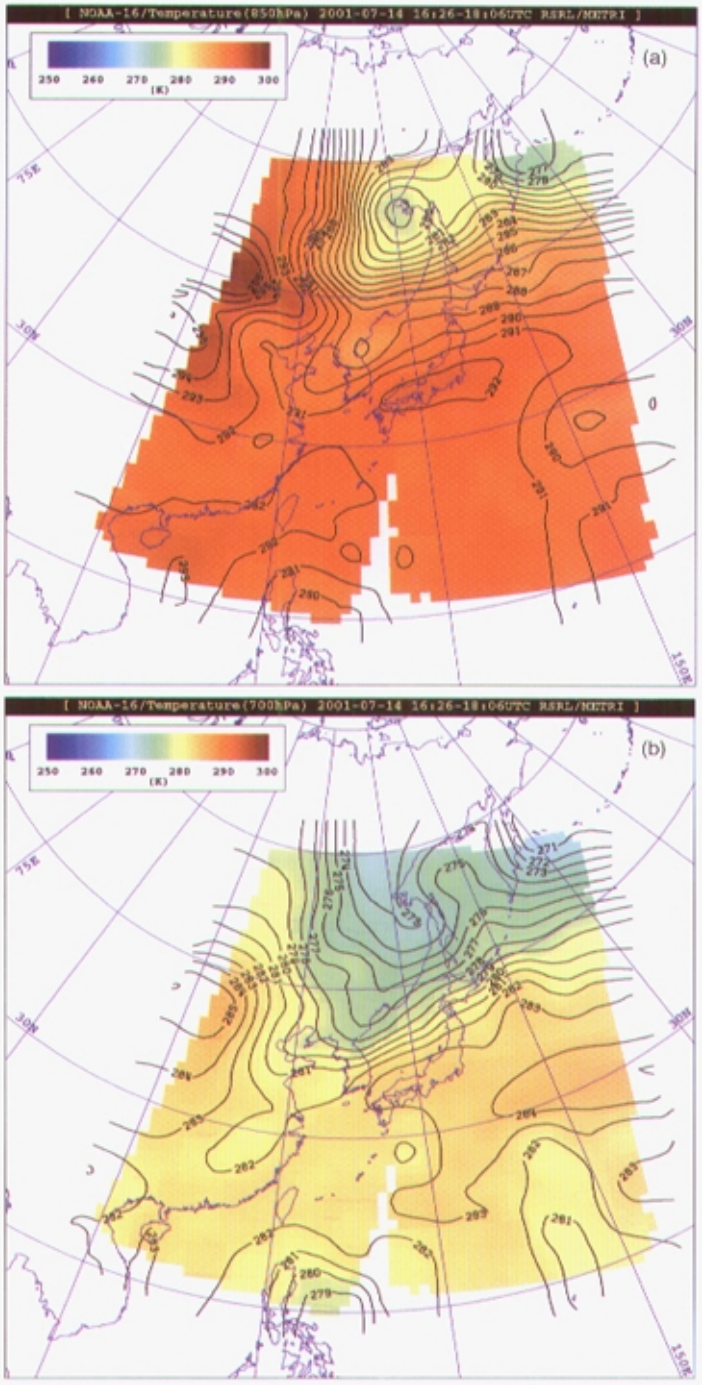

Fig. 3. An example of the temperature ((a) at 850 hPa, (b) at 700 hPa) and dew point temperature ((c) at 850 hPa, (d) 700 hPa) obtained from NOAA-16/ATOVS on 14 July 2001.

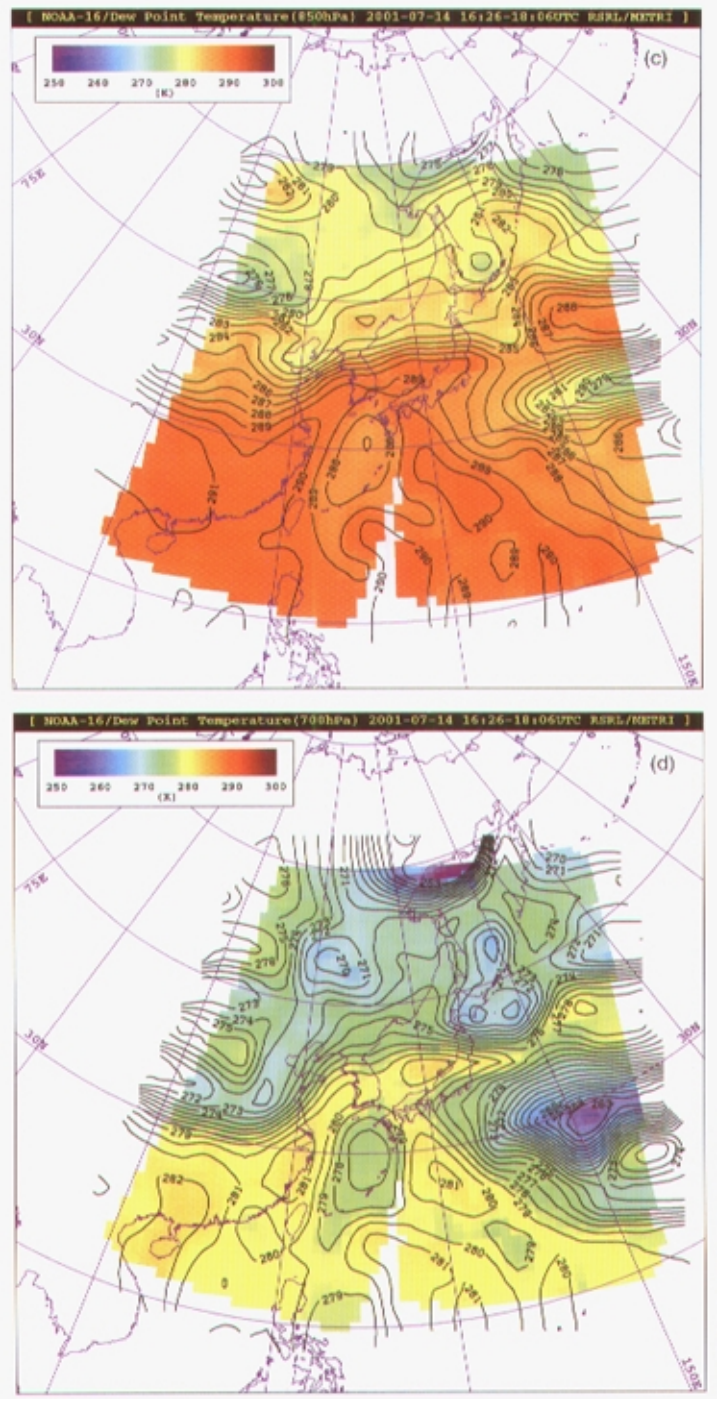

Fig. 3. (Continued).

The number of retrieved profiles for each morning and afternoon orbit during 2001 is shown in Fig. 4. The average number of orbits for each morning and afternoon pass is about two. The average number of profiles retrieved for each morning and afternoon orbit is about 1300 points, while in some cases the count exceeds more than 1500 points when the received number of orbits is 3. In comparison, the available number of radiosonde observation data for 0600 and 1800 UTC is only about 20, so the satellite-derived data could provide significant information. Furthermore, the ATOVS products provide much more information over the ocean where almost no radiosonde observations are made.

The spatial distribution of the number of retrieved profiles for one month, August 2001, is shown in Fig. 5. As the calibration is made at a regular scan number, the missing data points due to the calibration is also visible in the monthly composite image. Also, the maximum number of retrieved profiles for one month does not exceed more than 50 simply because of the presence of precipitation clouds, in which case the retrieval is not made. Although the aerial coverage varies with satellite orbit, the majority of the data is concentrated within ±23° of the receiving station, which is located around the center of the Korean Peninsula. The maximum coverage of data extends from 12°S to 60°N, and 90°E to 165°E, although the amount of information is limited.

4.2 *Results*

The retrieved temperature and dew point temperature profiles from the IAPP are compared with the radiosonde observations for the period of 10 May 2001 to 31 December 2001 over the stations in the East Asia region. Usually, most of the upper weather stations obtain the radiosonde data at 00 and 12 UTC, although some stations over the East Asia region, including the Osan upper-weather station in Korea, obtain additional data at 06 and 18 UTC. The total number of upper weather stations obtaining data at 06 and 18 UTC within the coverage of direct broadcast NOAA-16 data is only about 20 and the frequency of 6 hourly observation is fairly limited. As the radiosonde data are reported at different pressure altitudes from those of the IAPP standard altitude, the radiosonde data are linearly interpolated to the IAPP pressure altitudes. However, as there are many cases of missing data above 100 hPa altitude, we only compared the data from the ground to 100 hPa.

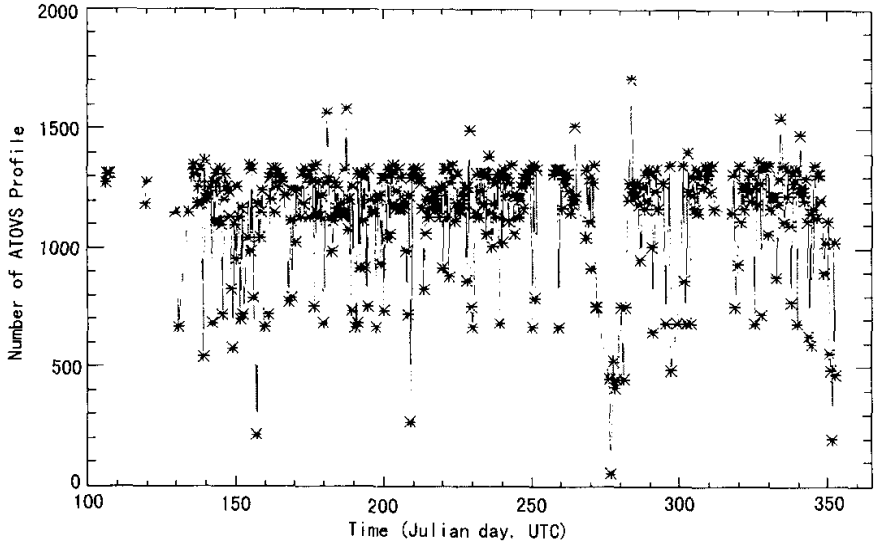

Fig. 4. Time series of the retrieved data points for each morning and afternoon orbit. The mean number of data points is about 1,300.

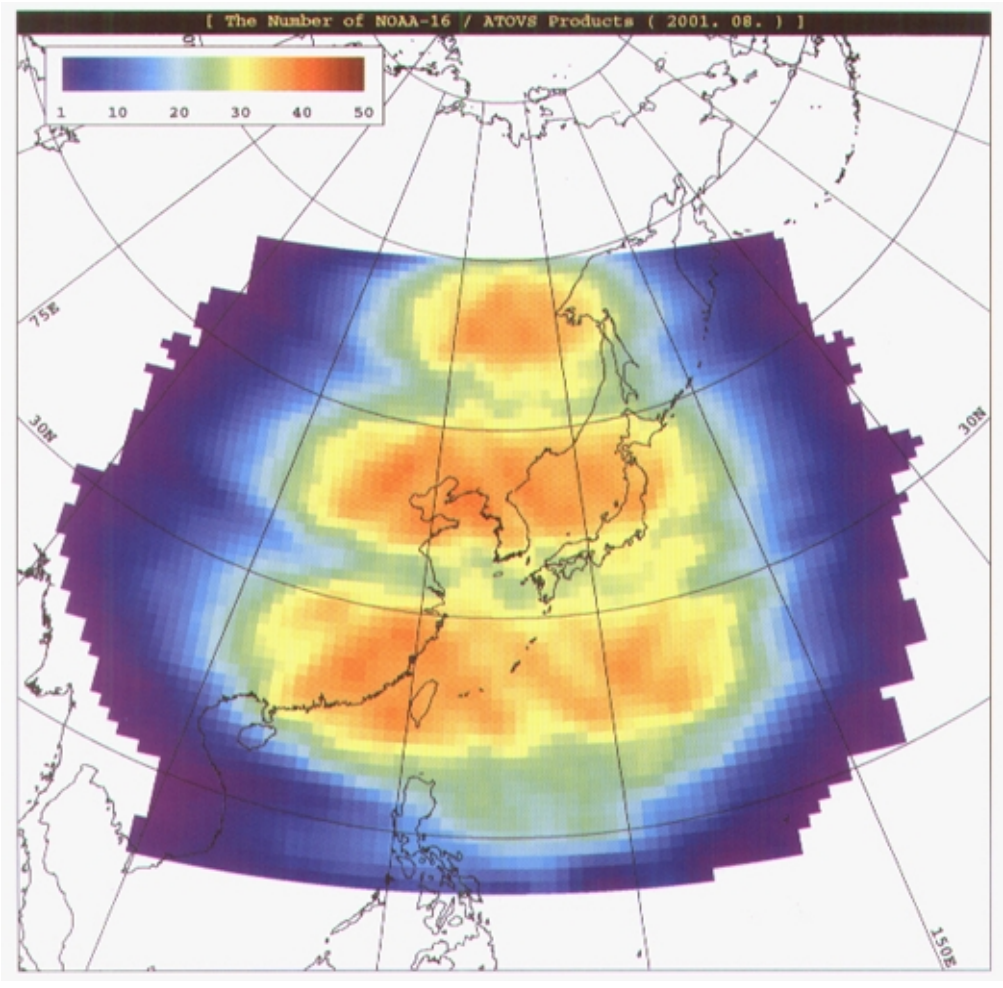

Fig. 5. The number of the retrieved points accumulated for one month, August 2001.

The first step for the validation is the construction of a match-up, both in time and space, data set. Due to the time difference between satellite pass and radiosonde observations, the number of match-up data sets is very small if the allowed time difference between the satellite and radiosonde observations is too small. Thus we chose three hours for our window to minimize the discrepancy and maximize the number of match-up data sets. Also, for the spatial window, we choose 1° based on the analysis done by Kim et al. (2001).

Figure 6 shows the vertical distribution of RMSE and bias averaged for all stations for 06 UTC and 18 UTC. The dash dot, dashed and solid lines are for clear, cloudy, and all- sky conditions, respectively. The total number of data points is 118 and 429 for clear and cloudy conditions, respectively. At the lower altitudes, below about 400 hPa, biases for the clear sky are slightly less than for the cloudy sky by about 0.2°C, while they are almost the same or slightly worse at the higher altitudes. Overall, bias is smaller at lower altitudes, about 0.5°C below about 600 hPa altitude, and larger at higher altitudes, at around 0.8°C. Simi-

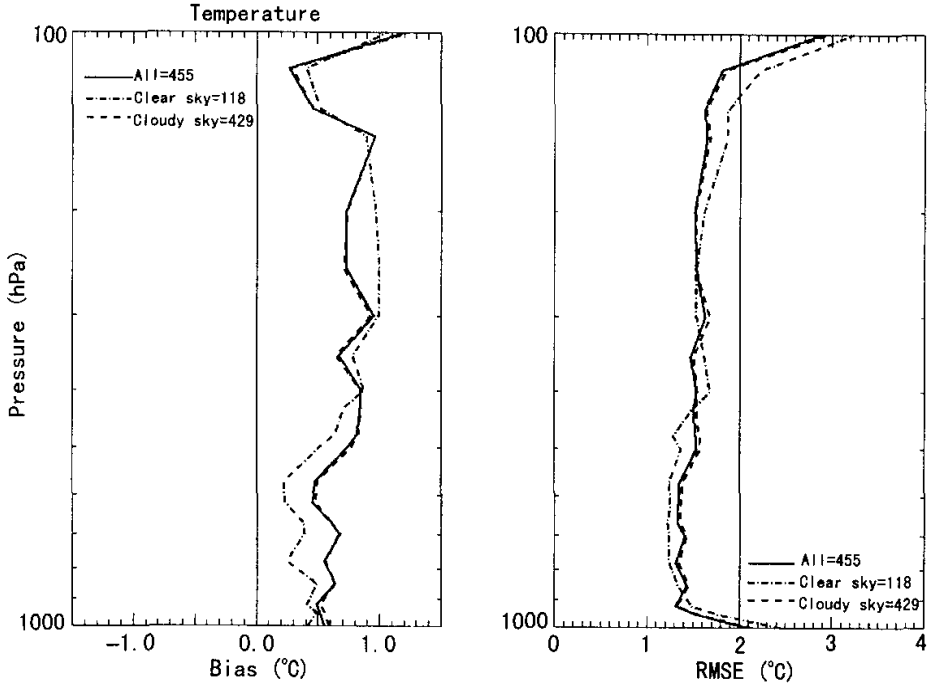

Fig. 6. Vertical distribution of (a) bias and (b) RMSE of the retrieved temperature as a function of altitude for the different sky conditions, clear (dash dot) and cloudy (dashed). The number of data points used for the estimations are 118 and 429 for clear and cloudy, respectively.

larly. RMSE is smaller for clear skies, especially at lower altitudes, although the difference is not significant. The overall value is better than 1.5°C at most altitudes, except near the ground and at the tropopause. Compared to the previous results from TOVS (Chung and Lee, 1999; METRI, 1991), the improvement of bias and RMSE is about 0.2 to 0.3°C. The major reason for the improvement is thought to be due to the improvement in the instruments and first guess profiles.

The error statistics are further analyzed for different surface conditions, over ocean and land. To separate land and ocean data, we first consider that the radiosonde stations in isolated islands represent the ocean environment. For the data obtained at the stations near the coastal area, we separate ATOVS data into land and ocean, depending on the retrieval position. The total number of collocated data sets for ocean and land is 249 and 311, respectively, and Fig. 7 shows bias and RMSE at different altitudes for land and ocean data. Overall, the bias and RMSE values over the ocean are smaller than those over land, especially near the ground and at altitudes higher than about 400 hPa. For example, the bias near the surface for the ocean is near 0°C, while it is about 1°C over land. At higher altitudes, the bias over the ocean is better than over land by at least 0.4°C. The RMSE near the ground is much better for the ocean surface than land by more than 0.5°C at an altitude of 975 hPa.

To check the stability of the procedure with time, we analyze the temporal variation of the error statistics. Figure 8 shows the time series of the monthly mean and standard deviation of the residual defined as the temperature difference between radiosonde observation and ATOVS retrieval at four different altitudes, 300, 500, 850, and 950 hPa. Numbers below the symbols represent the number of data points used for the calculation. A positive residual is consistently shown for all months, which implies that the accu-

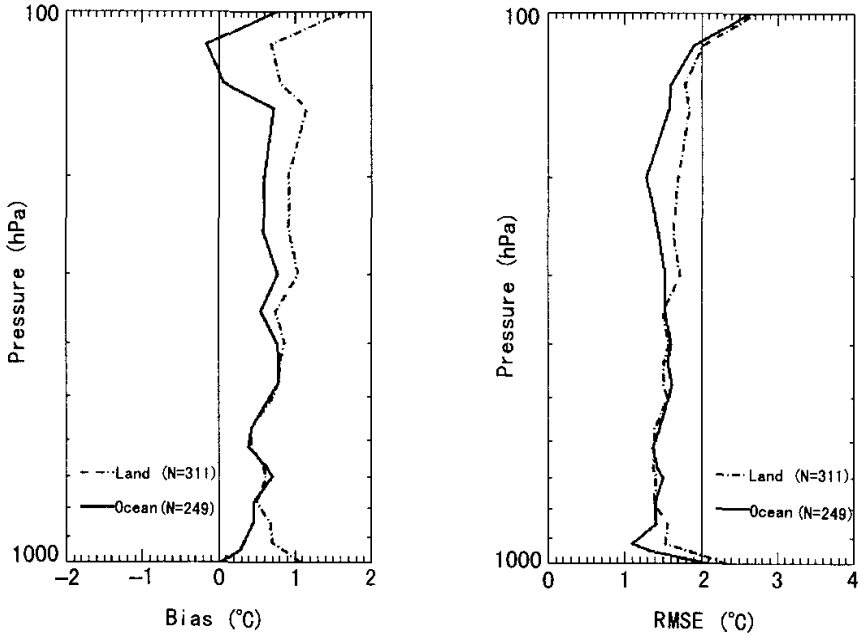

Fig. 7. Same as Fig. 6 except for different surface conditions, ocean (blue) and land (red). The number of data points used for the estimations are 249 and 311 for ocean and land, *respectively.*

racy of the retrieved temperature is fairly consistent with time. This is also true for the standard deviation of the residual, which is better than 1.5°C, except for the large value for June at altitudes of 300, 850, and 950 hPa. Thus, we can be assured the overall error statistics do not change significantly with season.

Figure 9 shows the validation result of the water vapor mixing ratio. Contrary to the temperature profile. there is a clear distinction between the clear and cloudy sky conditions. The overall results are much better for clear sky conditions than for cloudy conditions. For example, the bias is about 0.3 g kg^{-1} for clear skies, while it is more than 0.5 g kg^{-1} for cloud conditions at lower altitudes. Similarly, the RMSE at 900 hPa is about 1.0 g kg^{-1} for clear skies and about 1.3 g kg^{-1} for cloudy conditions. The difference is thought to be due to the insufficient correction of cloud effects on the water vapor channels and to the difficulty in the retrieval of water vapor for cloudy areas. Although the overall performance of water vapor retrieval is worse than that of temperature, the spatial distribution of the high-resolution data could provide critical information for the influx of water vapor into a certain area. Similar to the temperature case, there is no significant temporal variation of the error statistics (not shown).

5. Discussions and conclusion

Operational procedures to retrieve the vertical profiles of temperature and dew point temperatures from NOAA-16/ATOVS data using AAPP and IAPP have been implemented in KMA since May 2001. AAPP is used for the post-processing of direct readout ATOVS data, which generates geo-located and calibrated level 1d data files. The actual retrieval is made through the IAPP package, which uses the level 1d ATOVS data with several ancillary data such as the model-predicted surface temperature and vertical profiles of temperature and humidity as a first guess. The current procedures consist of the version 3 of AAPP and version 2 of IAPP and use the NCEP Aviation model forecast fields for the first guess. The number of data points from NOAA-16/ATOVS data for each morning

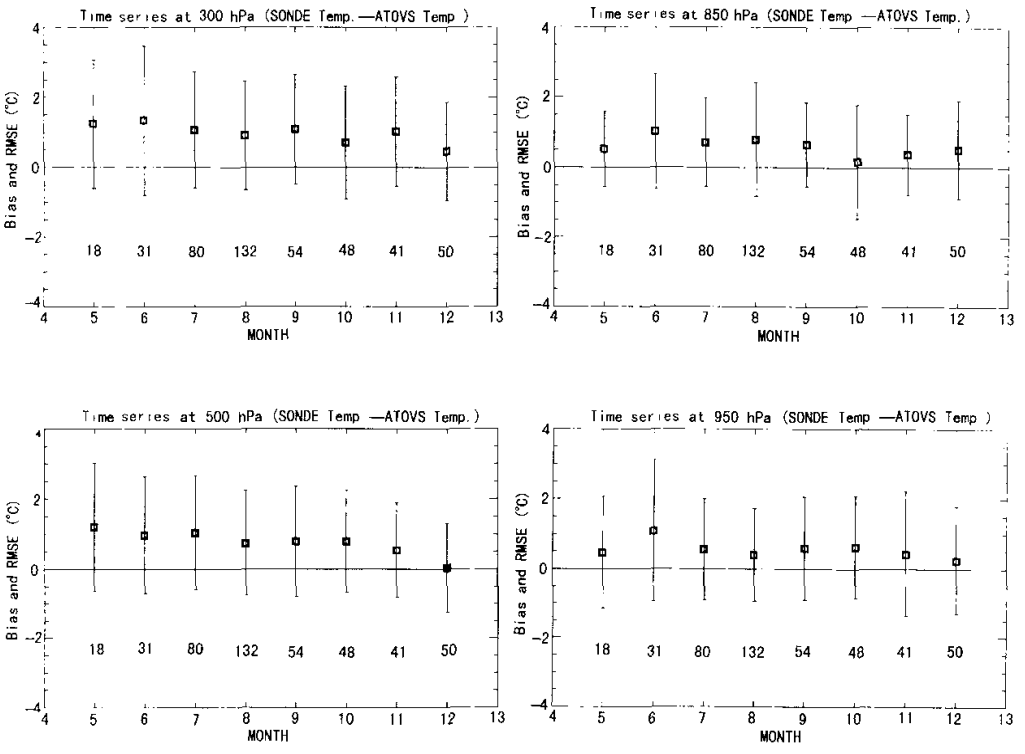

Fig. 8. Same as Fig. 6 except for different surface conditions, ocean (solid) and land (dash dot). The number of data points used for the estimations are 249 and 311 for ocean and land, respectively.

and afternoon orbit is about 1300, which is much larger than that of the radiosonde observation, which is only about 20. The retrieved fields of temperature and dew point temperature could be used even for nowcasting through providing upper air information for the time when the ground-based data is void.

The products, temperature and dew point temperature (equivalently water vapor mixing ratio), derived from the direct readout data at KMA are validated with the collocated radiosonde data. For the collocation, we use a time and space filter of 3 hours and 1°. The validation results show that the retrieved temperature has a positive bias with RMSE of about 1.5°C. Although there is no significant difference in the error statistics in the temperature profiles for cloudy and clear skies, the water vapor mixing ratio is much better in clear sky conditions, especially at lower altitude. For different surface conditions, ocean versus land, the most significant difference is shown at the lower levels and upper levels, higher than about 400 hPa altitude. Especially near the ground, the bias and RMSE values over the ocean are much better than those over land, which could be attributed to the uncertainties in the emissivity information of the land surface.

Currently, the match-up data set is being used to construct a bias correction table for each of the HIRS/3 and AMSU channels. The bias correction value will be ultimately re-used in the retrieval procedure. Also, to enhance the spatial resolution of the retrieved values, one pixel retrieval method is under development.

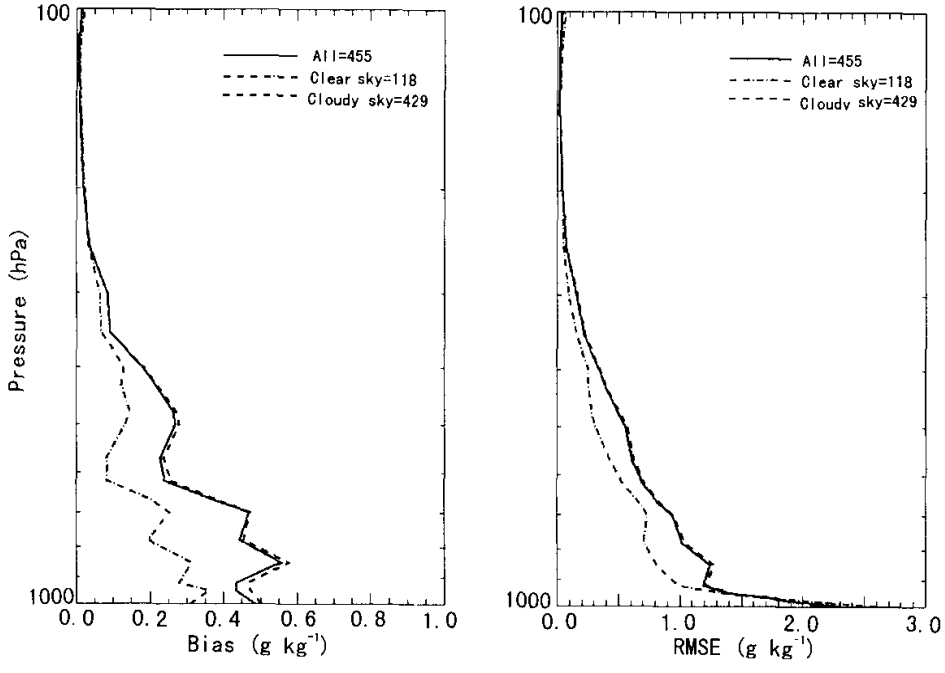

Fig. 9. Same as Fig. 6 except for the water vapor mixing ratio.

Acknowledgments. We wish to thank two anonymous reviewers for their careful reviews. This work was supported by the project "Development of Monitoring and Prediction Technology for Severe Weather (Heavy Rainfall) over the Korean Peninsula" of the Korea Meteorological Administration.

REFERENCES

Barcilon, V., 1975: On Chahine's relaxation method for the radiative transfer equation. *J. Atoms. Sci.*, **32**, 1626–1630.

Chahine, M. T., 1968: Determination of the temperature profile in an atmosphere from its outgoing radiance. *J. Opt. Soc. Amer.*, **58**, 1634 1637.

Chahine, M. T., 1970: Inverse problems in radiative transfer: A determination of atmospheric parameters. *J. Atmos. Sci.*, **27**, 960–967.

Chung, H. S., and Y. S. Lee, 1999: ITPP-5.12 retrieval on McIDAS system. *Technical Proceedings of the Tenth International ATOVS Study Conference*, Boulder, Colorado, 99–103.

Deepak, A., H. E. Fleming, and M. T. Chahine, 1985: *Advances in Remote Sensing Retrieval Methods*. A. Deepak Publ. Hampton, VA. U.S.A., 737 pp.

Fleming, H. E., 1977: Comparison of linear inversion methods by examination of the duality between iterative and inverse matrix methods. *Inversion Methods in Atmospheric Remote Sounding*. A. Deepak, Ed., Academic Press, 325–355.

Fleming, H. E., and W. L. Smith, 1971: Inversion techniques for remote sensing of atmospheric temperature profiles. *Fifth Symposium on Temperature*, Instrument Society of America, Pittsburg, Pennsylvania, 2239–2250.

Kim, M. J., M. H. Ahn, C. Y. Chung, and A. S. Suh, 2001: Retrieval and validation of temperature using the NOAA-16/ATOVS data near the Korean Peninsula. *Proceedings of Korea Meteorological Society Fall Meeting*, 274–277.

Le Marshall, J., R. Seecamp, G. Mills, and K. Magari, 1995: Operational assimilation of TOVS radiance data in the Australian Bureau of Meteorology. *Technical Proceedings of the Eighth International TOVS Study Conference*, Queenstown, New Zealand, 335–346.

Le Marshall, J., R. F. Davidson, M. C. Willmott, and P. E. Powers, 1989: A physically based operational atmospheric sounding system for the Australian Region. *Aust. Met. Mag.*, **37**, 193–199.

Li, J., and H. L. Huang, 1999: Retrieval of atmospheric profiles from satellite sounder measurements using the discrepancy principle. *Appl. Opt.*, **38**, 916–923.

Li, J., W. W. Wolf, W. P. Menzel, W. Zhang, H. L. Huang, and T. H. Achtor, 2000: Global sounding of the atmosphere from ATOVS measurements: The algorithm and validation. *J. Appl. Meteor.*, **39**, 1248 1268.

Mateer, C. L., 1965: On the information content of Umkehr observations. *J. Atmos. Sci.*, **22**, 370–381.

Menzel, W. P., and A. Chedin, 1990: Summary of the Fifth International TOVS Study Conference, *Bull. Amer. Meteor. Soc.*, **71**, 691–693.

Meteorological Research Institute (METRI), 1991: A study on the comparison and calibration of TOVS data and analysis of upper air state over Korea by TOVS outputs. *MR 91-7*, 153 pp.

NOAA, 1988: Data extraction and calibration of TIROS-N/NOAA radiometers, NOAA Tech. Memo. NESS107, 52 pp.

NOAA, 1998: NOAA-KLM Uuser's Guide (http://www2.ncdc.noaa.gov/docs/klm), NOAA.

Rodgers, C. D., 1976: Retrieval of atmospheric temperature and composition from remote measurements of thermal radiation. *Rev. Geophys. Space Phys.*, **14**, 609–624.

Smith, W. L., 1970: Iterative solution of the radiation transfer equation for the temperature and absorbing gas profile of an atmosphere. *Appl. Opt.*, **9**, 1993–1999.

Smith, W. L., and H. M. Woolf, 1976: The use of eigenvectors of statistical covariance matrices for interpreting satellite sounding radiometer observations. *J. Atmos. Sci.*, **35**(7), 1127–1140.

Smith, W. L., H. M. Wolf, C. M. Hayden, D. Wark, and L. M. McMillian, 1979: The TIROS-N operational vertical sounder. *Bull. Am. Meteor. Soc.*, **60**, 1177–1187.

Smith, W. L., G. S. Wade, and H. M. Woolf, 1985: Combined atmospheric sounder/cloud imagery—A new forecasting tool. *Bull. Amer. Meteor. Soc.*, **66**, 138–141.

Smith, W. L., H. M. Wolf, S. J. Nieman, and T. H. Achtor, 1993: ITPP5—The use of AVHRR and TIGR in TOVS data processing. *Technical Proceedings of the Seventh International TOVS Study Conference*, Igls, Austria, 443–453.

Strand, O. N., and E. R. Westwater, 1968: Statistical estimation of the numerical solution of a Fredholm integral equation of the first kind. *J. Ass. Comput. Mach.*, **15**, 100–114.

Twomey, S., 1963: On the numerical solution of Fredholm integral equations of the first kind by the inversion of the linear system produced by quadrature, *J. Ass. Comput. Mach*, **10**, 97–101.

Weng, F., and N. Grody, 2000: Retrieval of ice cloud parameters using a microwave imaging radiometer. *J. Atmos. Sci.*, **57**, 1069–1081.